Acta of Bioengineering and Biomechanics
Vol. 24, No. 1, 2022

Original paper
DOI: 10.37190/ABB-01991-2021-05

A kinematic model of a humanoid lower limb exoskeleton with pneumatic actuators

SEBASTIAN GŁOWIŃSKI[1, 2]*, MARIUSZ PTAK[3]

[1] Koszalin University of Technology, Faculty of Mechanical Engineering,
Department of Mechatronics and Automatics, Koszalin, Poland.
[2] Pomeranian Academy is Słupsk, Institute of Health Sciences, Słupsk, Poland.
[3] Wrocław University of Science and Technology, Faculty of Mechanical Engineering,
Department of Machine Design and Research, Wrocław, Poland.

Purpose: Although it is well-established that exoskeletons as robots attached to the human body's extremities increase their strength, limited studies presented a computer and mathematical model of a human leg pneumatic exoskeleton based on anthropometric data. *Methods*: By using Inertial Measurement Units a lower limb joint angles (hip, knee and ankle in sagittal plane) during walking and running were calculated. The geometric model of a human leg pneumatic exoskeleton was presented. Joint angle data acquired during experiments were used in the mathematical model. *Results*: The position and velocity of exoskeleton actuators in each phase of the movement were calculated using the MATLAB package (Matlab_R2017b, The MathWorks Company, Novi, MI, USA). *Conclusions*: The obtained results demonstrate the efficiency of the proposed approach that can be utilized to analyze the kinematics of pneumatic exoskeletons using the dedicated design process. The developed mathematical model makes it possible to determine the position of lower limb segments and exoskeleton elements. The proposed model allows for calculating the position of the human leg and actuators' characteristic points.

Key words: *inertial measurement unit, exoskeleton model, kinematic, pneumatic exoskeleton, simulation*

1. Introduction

The development of robotics and computing power allows the designing of devices for amplifying human power. Mobile anthropomorphic robots are examples of the above-mentioned machines which assist in the operation of human muscles and are called exoskeletons [25], [27]. Exoskeleton gait rehabilitation systems present a new rehabilitation method for patients [28]. They provide overall controllable-level assistance for gait rehabilitation and reduce therapist workload and therapy costs [15], [18]. Wearable robotics or exoskeletons have unique sets of design requirements. For example, Valayil and Augustine proposed a serial-parallel hybrid manipulator for rehabilitation of upper limb in stroke-affected patients [33]. According to the authors, this type of manipulators has a good kinematic characteristics while performing wrist motions. Exoskeletons devices must be portable, safe and lightweight [39]. Electric motors with gears, hydraulic actuators and pneumatic muscles are used as the executive systems of exoskeletons [14], [31]. Pneumatic muscles have special characteristics that render it optimum for medical equipment developed for patient rehabilitation by continuous passive motion [24]. The procedure for selecting pneumatic actuators can also be found in [17], [30].

The manufacturing cost is lower because low-cost pneumatic actuators drive the pneumatic-driven robot

* Corresponding author: Sebastian Głowiński, Koszalin University of Technology, Faculty of Mechanical Engineering, Department of Mechatronics and Automatics, ul. Śniadeckich 2, 75453 Koszalin, Poland. Phone: +48 94 3478395, e-mail: sebastian.glowinski@tu.koszalin.pl
Received: November 23rd, 2021
Accepted for publication: February 11th, 2022

gait exoskeletons. The advantage of pneumatic systems is their lightweight, cleanness and safety. A wide variety of pneumatic muscle types was described by Caldwell et al. [3] and Daerden et al. [4]. Unfortunately, the pneumatic-driven robot gait rehabilitation system exhibits very complicated motion and is difficult to be modelled mathematically [26], [34]. Its dynamics are related to air pressure, load changes, temperature changes and external disturbances [35].

Some exoskeleton publications presented a diagram of a wearable system [38]. In this paper, we present an exact geometric model that can be useful for designers. Thus, this study aimed to create a mathematical model for a pneumatic exoskeleton.

The remainder of this paper is organized as follows. In Section 2, the gait kinematic parameters were obtained using Inertial Measurement Units (IMUs). The procedure was presented in previous works by Głowiński et al. [6], [7]. Based on the orientation of IMUs, the angles in the individual joints of the lower limb in the sagittal plane were acquired. Next, the basic model of the pneumatic exoskeleton in the sagittal plane is presented. Then, the coordinates of the exoskeleton and human leg characteristic points as a mathematical explanation are established gradually. The proposed mathematical models are built as a function of human height. This method allows determining the location of characteristic points of the wearable system. The angle values obtained during the experiment were implemented in the model. The equations of the kinematics of the wearable system are presented, and the experimental results are described. Finally, a brief conclusion with some limitations of the study is presented.

2. Materials and methods

2.1. Lower limb parameters (walk and run)

Our research was divided into two parts (Fig. 1a). The first one was the IMU experiment and exoskeleton model with data processing and simulation. Twenty-six subjects (male = 14, female = 12) participated in this study. The Bioethics Committee approved the study protocol at the district medical chamber in Gdańsk – Poland (KB-14/20). Before the study, the investigator explained all procedures in detail to the subjects. The acceptance rate was 100%, so all subjects agreed to wear the sensors and participate in the experiment. The participants' mean age (SD – standard deviation) was 22.8 years (0.79), mean height was 169.45 cm (8.26), and mean body weight was 68.05 kg (9.27), respectively. All the tested subjects walked and ran on a flat surface at the speed they preferred. Stability during gait and run is a factor influencing speed selection. Individuals use energetically suboptimal gaits when walking. The people may instead be choosing gait parameters that maximize stability while walking. Individual joint and muscle biomechanics also directly affect walking speed. Thus, due to the research we have decided to choose the preferred speed [11], [22]. The research equipment included a ProMove mini platform with mini sensors (Inertia Technology, 2021). This device consists of a wireless network to transfer data to a computer. Thus, the data were analyzed in real-time.

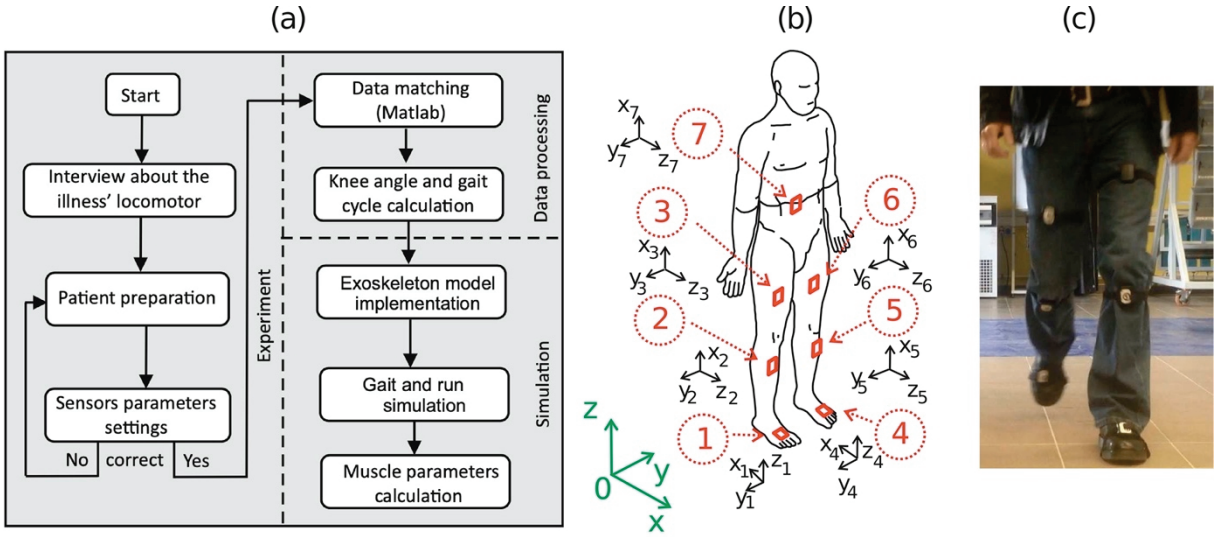

Fig. 1. (a) Flowchart of the experimental procedure; (b) the human model and coordinate systems; (c) a subject wearing the ProMove mini nodes

By using ProMove mini sensors, it is possible to record data in continuous time. Each sensor has built-in memory 2 GB (2 gigabytes), which allows it to write data up to 7 h. The device contains triaxial accelerometers, gyroscopes, and magnetometers. All channels are sampled at 1000 Hz. The range of accelerometers is ±16 g, and the range of the gyroscopes is to 2000 deg/s. The flash memory of each sensor is has the low-power RF (radio-frequency) transceiver is in the 2.4 GHz license-free band. Because of the ergonomic design, the ProMove sensors can be easily attached to the body with a strap. Each sensor is 51 mm (length) to 46 mm (width) and 15 mm (height) in size. The sensor mass is 20 grams (including batteries). Data collection <100 ns is synchronized by an Inertia gateway as the central hub connected to a personal computer via a USB (Universal Serial Bus). All data (experimental samples, orientation as Euler angles or quaternions, acceleration along three axes and angular velocities) are downloaded by the Inertia Studio package. Next, they are recorded for further analysis. During the experiment, sensors were placed along the right and left legs, more specifically on the thigh, lower leg, and foot (Fig. 1b, c). The X, Y, Z coordinates represent the global coordinate system, the x_s, y_s, z_s represent the sensor coordinate system. In a global coordinate system, the X-axis is the moving direction and the Y-axis is the lateral direction. The Z-axis presents the opposite direction of gravity [5]. The orientation of each sensor is calculated relatively to the Earth's reference frame. As a result, roll, pitch and yaw sensor angles are acquired. Based on the orientation of each sensor, the angles in the individual joints of the lower limb in the sagittal plane were acquired. A fundamental problem in IMU-based human motion analysis is that the IMUs' local coordinate axes are not aligned with any physiologically meaningful axis. It is very difficult to attach IMUs to the leg in such a way that one of the local coordinate axes coincides exactly with the knee joint axis. The body straps that we used to attach IMUs to the leg yield an almost arbitrary orientation of the IMU towards its segment (Fig. 1c). Thus, the hinge joint angle can be calculated from the inertial measurement data. But the data from both sensor units must be transformed into joint-related coordinate systems (coordinate systems in which one or two axes coincide with the joint axis and/or the longitudinal axis of the segment). From a user's point of view, more convenient case of arbitrary mounting orientation, it is required to identify the joint axis coordinates in the local coordinate systems of the sensors attached to both ends of the joint. For example, a joint coordinate system (JCS) was proposed by the Standardization and Terminology Committee (STC) of the International Society of Biomechanics [37]. After experiments, hip, knee, and ankle motions were calculated by the orientation of each segment (thigh, shank and foot). Next, these were described in the XYZ-Euler angle representation [13]. IMUs were placed on the parallel plane to the anteroposterior plane. The proposed exoskeleton model works in the sagittal plane, and, therefore, we based our calculations only on the angles in the sagittal plane. For example, if we want calculate the knee angle (right leg) we choose two IMUs (3 and 2nd). They contain 3D accelerometers and 3D gyroscopes. These sensors are forming two sensor frames x_3, y_3, z_3 and x_2, y_2, z_2. The knee joint X, Y, Z is recommended by international society of biomechanics in a mutual coordinate system. Next step is the transformation from the initial sensor frames into the JCS (X, Y, Z-Euler angle representation). Thus, the sensor frames were transformed into a joint/mutual coordinate system (JCS) to compute the hip, knee and ankle angles. The multiplication of the single rotation matrices around each axis transforms the sensor frame at any time step into the initial sensor frame. The rotation matrices are determined by the equation (1)

$$\mathbf{R}_i = \begin{bmatrix} c\theta c\psi & -c\theta s\psi & s\phi \\ c\phi c\psi + s\phi s\theta c\psi & c\phi c\psi - s\phi s\theta s\psi & -s\phi c\theta \\ s\phi s\psi - c\phi s\theta c\psi & s\phi c\psi + c\phi s\theta s\psi & c\phi c\theta \end{bmatrix}, \tag{1}$$

where c and s denote the cos and sin function and φ, θ, and ψ are the rotation angles about x_s-, y_s-, and z_s-axes, respectively [36].

After collecting all data from the IMUs, they were imported using MATLAB. We obtain a signal consisting of several steps. Next, the beginning of each step (the left and right legs) was determined. Because some of the steps consist of 200–240 samples (different number of samples) it was necessary to interpolate every step by using Curve fitting – Matlab toolbox. Subsequently, we performed every step consisting of 100 samples. This implied that the data were transformed into a gait cycle. Finally, the left and right angles were calculated (an average of 30 steps).

2.2. Exoskeleton of the lower limb with pneumatic muscles

The pneumatic exoskeleton designed in this work can provide assistive force to hip, knee joint flexion and also to ankle plantar flexion [9]. Exoskeleton can be used mainly to reduce muscle fatigue during a human

walk. The braces, cuffs, straps and orthopaedic components can be used to attach exoskeletons to a human limb. For example, Valayil et al. [33] proposed using a hybrid manipulator to perform human wrist motions and elbow motions during rehabilitation therapy for upper limb in stroke-affected patients. By using velcro strapping, they obtain the desired alignment, thereby preserving the natural movement of the human arm. The procedure for selecting pneumatic actuators can also be found in [17], [30]. To support the movement of the lower limb, the six pneumatic muscles were proposed (movement only in saggital plane). The first phase (loading response of 0–12% of a gait cycle) is a period of extensive muscle activity. Hip flexion is controlled by isometric action of the hamstrings and gluteus maximus. The quadriceps act eccentrically to control knee flexion, whereas the ankle dorsiflexors act eccentrically to prevent slapping of the foot on the ground. In midstance (12–31% of gait cycle) the quadriceps act concentrically to initiate knee extension, whereas in ankle, the intrinsic muscles activate to convert the foot into an increasingly rigid structure. In terminal stance (31–50% of gait cycle), the plantar flexors maintain knee extension. The hip abductors move from eccentric to isometric to concentric activity, elevating the pelvis in preparation for swing. The iliopsoas becomes active, eccentrically controlling the rate of hip extension. The ankle plantar flexors become isometric at 35 to 50% of gait cycle. Next, they continue forward momentum in the body's upper part causes the heel to rise from the ground. In preswing (50–62% of gait cycle) the plantar flexors act concentrically, producing a propulsive push off. The iliopsoas shifts from eccentric to concentric activity which will advance the extremity into swing phase. The rectus femoris limit knee flexion and augment hip flexion. The erector spinae are active on the preswing side. In initial swing phase, hip flexors and knee extensors continue their preswing activity. The dorsiflexors act concentrically to permit the forefoot to clear the ground. The hip adductors can also assist during preswing and initial swing to assist in hip flexion. In therminal swing phase, the hamstrings act eccentrically to decelerate the swinging extremity. The dorsiflexors hold the ankle in position for initial contact. Just before the foot touches the ground, the quadriceps and the hip abductors initiate activity. The body prepares for the large ground reaction its joints will encounter at initial contact.

The kinematic diagram of the experimental model of the lower limb exoskeleton with actuators (paraller to selected parts of muscles) is presented in Fig. 2a. Muscles 1 – great gluteus (gluteus maximus), 2 – iliopsoas (musculus iliopsoas), are responsible for straightening and bending the hip joint. The 3 – hamstring and 4 – quadriceps muscles (vastus lateralis) support the bending and straightening of the lower leg. 5 – gastrocnemius muscles and 6 – tibialis anterior muscles (tibialis anterior) have been proposed for flexing and extending the ankle joint. In fact, the iliopsoas muscle is attached to the spine. In two-way movements, a pair of antagonist muscles were used. Muscle pairs 1–2, 3–4, 5–6 have two input signals – pressure (p), and one output in driving torque (τ). For example, the moment generated by a pair of muscles 1–2 in the hip joint, as the sum of three components can be expressed by the relationship:

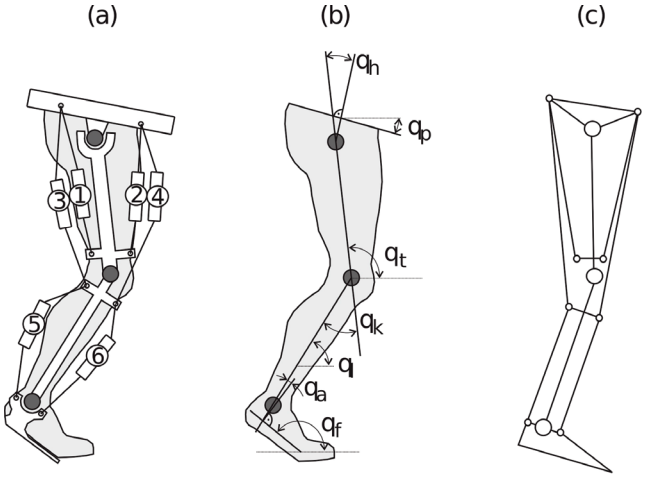

Fig. 2. (a) Pneumatic model of the exoskeleton of the lower limb; (b) angles of selected joints; (c) computer model

$$\tau = k_1(p_1 - p_2) + k_2\theta_h^2(p_1 - p_2) - k_3\theta_h(p_1 + p_2). \quad (2)$$

The first component of Eq. (2) characterizes the ability to control the system by changing the pressure, the second one results from the non-linearity of the muscle characteristics and the third component is a function of the stiffness of the drive proportional to the sum of the pressures in both muscles. The coefficients k_1, k_2, k_3 can be determined experimentally.

The mobility of the proposed model is defined as $w = 3$, that is, to fix the position or immobilize all the elements of the exoskeleton, it is enough to know three parameters. These can be hip θ_h, knee θ_k and ankle θ_a angles, respectively. It is possible to define three angles by specifying the length of the muscles in eight selected configurations: (1, 3, 5), (1, 3, 6), (1, 4, 5), (1, 4, 6), (2, 3, 5), (2, 3, 6), (2, 4, 5) and (2, 4, 6). The change in the length of the muscles during movement is known as local mobility. In order to determine the hip flexion θ_h, knee θ_k and ankle θ_a, the following relationships should be used (Fig. 2b):

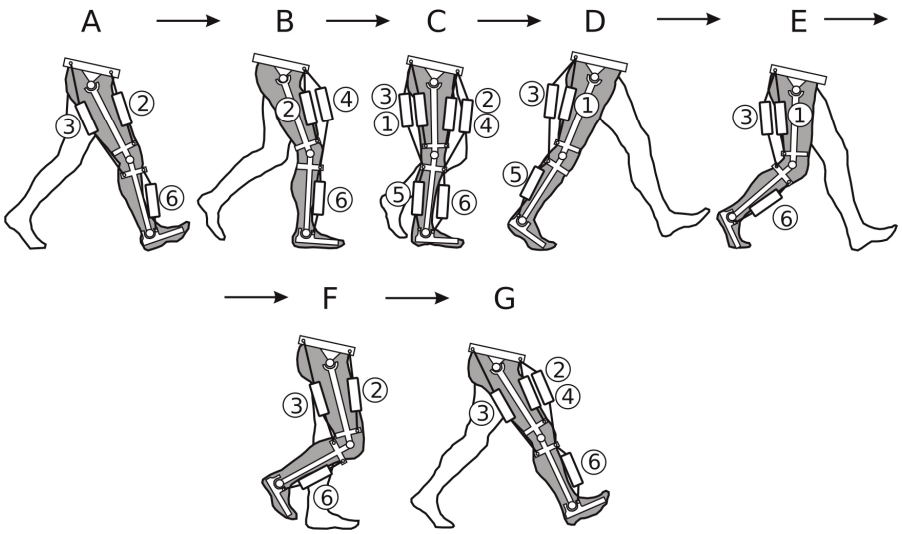

Fig. 3. Muscle activity in individual phases of one step

$$\begin{aligned} \theta_h &= \theta_t - \theta_b && 5° \le \theta_h \le +125° \\ \theta_k &= \theta_t - \theta_l && \text{, where } 0° \le \theta_k \le +130° \\ \theta_a &= \theta_f - \theta_l - 90° && -10° \le \theta_a \le +60° \end{aligned} \quad . \quad (3)$$

Walking involves all the joints of the lower limb. An effective gait requires a complex interplay between agonist versus antagonist muscles. The activity of exoskeleton muscles during one step in particular phases is illustrated in Fig. 3. The thigh acceleration while walking is achieved thanks to the iliopsoas and the rectus muscles of the thigh. Decelerating during movement is obtained thanks to the hamstring muscles' eccentric tension (lengthening) entering the hip joint. The task of the anterior shin group muscles is to lower the foot towards the ground when the heel hits it. The quadriceps muscle absorbs energy and prevents the knee from bending. Upon impact with the foot on the ground, abductors tighten to keep the torso upright. The triceps muscles of the calf, which include gastrocnemius, soleus and plantar muscles, are responsible for shifting the centre of gravity of the body forward. When the toes are lifted, the quadriceps muscle flexes concentrically to support the plantar flexors of the foot, push the body forward and lengthen the stride [2]. A detailed mathematical description of gait with a model of dynamics in individual phases can be found, among others, in [16], [20], [21], [23], [25].

The analysis of the kinematics of the pneumatic exoskeleton should begin with the determination of the constant parameters. On this basis, the coordinates of characteristic points should be determined. Some of them are constant, such as points A, B, C, but point D_0, ..., O_0 are initial position (standing as in Fig. 4).

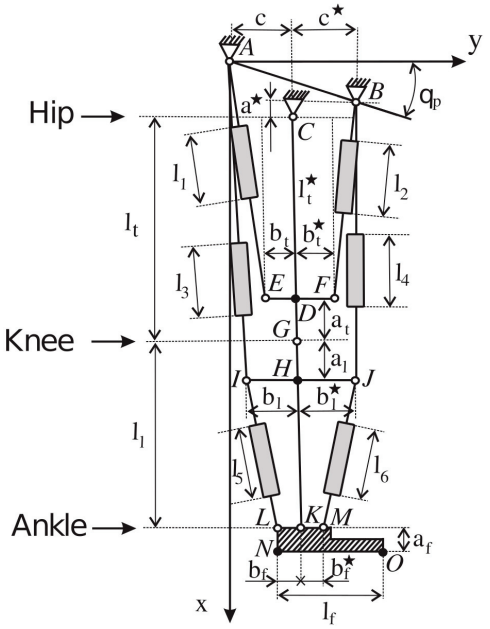

Fig. 4. Structural diagram with the parameters of the pneumatic exoskeleton model of the lower limbs

In the starting position (the thigh bone and the lower leg is directed vertically downwards, the foot is horizontal), the coordinates of fixing the muscles with the tendons are determined. The coordinates of the characteristic points in the adopted system in the initial position (as in Fig. 4) are calculated as:

$$A = (0, 0),$$

$$B = ((c + c^*)\tan\theta_p, c + c^*),$$

$$C = ((c + c^*)\tan\theta_p + a^*, c),$$

$$D_0 = ((c + c^*)\tan\theta_p + a^* + l_t - a_t, c),$$

$$E_0 = ((c+c^*)\tan\theta_p + a^* + l_t - a_t, c - b_t),$$

$$F_0 = ((c+c^*)\tan\theta_p + a^* + l_t - a_t, c + b_t^*),$$

$$G_0 = ((c+c^*)\tan\theta_p + a^* + l_t, c),$$

$$H_0 = ((c+c^*)\tan\theta_p + a^* + l_t + a_l, c), \qquad (4)$$

$$I_0 = ((c+c^*)\tan\theta_p + a^* + l_t + a_l, c - b_l),$$

$$J_0 = ((c+c^*)\tan\theta_p + a^* + l_t + a_l, c + b_l^*),$$

$$K_0 = ((c+c^*)\tan\theta_p + a^* + l_t + l_l, c),$$

$$L_0 = ((c+c^*)\tan\theta_p + a^* + l_t + l_l, c - b_f),$$

$$M_0 = ((c+c^*)\tan\theta_p + a^* + l_t + l_l, c + b_f^*),$$

$$N_0 = ((c+c^*)\tan\theta_p + a^* + l_t + l_l + l_a, c - b_f),$$

$$O_0 = ((c+c^*)\tan\theta_p + a^* + l_t + l_l + l_a, c + l_f - b_f).$$

Knowing the distances, it is possible to choose the length of the muscles at rest l_{10}, l_{20}, ..., l_{60}, and to determine the length of the strings themselves l_{10}^*, l_{20}^*, ..., l_{60}^*, with which the muscles are attached to the exoskeleton frame. During the operation of the exoskeleton, changing the length of the tendons themselves is ignored. Based on equation (4), the length of the tendons themselves in the initial position is determined from the equation:

$$l_{10}^* = \sqrt{(c - b_t)^2 + ((c+c^*)\tan\theta_p + a^* + l_t)^2} - l_{10},$$

$$l_{20}^* = \sqrt{(c - b_t^*)^2 + (a^* - a_t + l_t)^2} - l_{20},$$

$$l_{30}^* = \sqrt{(c^* - b_l)^2 + ((c+c^*)\tan\theta_p + a^* + l_t + a_l)^2} - l_{30}, \qquad (5)$$

$$l_{40}^* = \sqrt{(c^* + b_l^*)^2 + (a^* + a_l + l_t)^2} - l_{40},$$

$$l_{50}^* = \sqrt{(b_l - b_f)^2 + (l_l - a_l)^2} - l_{50},$$

$$l_{60}^* = \sqrt{(b_l^* - b_f^*)^2 + (l_l + a_l)^2} - l_{60}.$$

To determine the location of characteristic points, directional cosine matrices can be used, which in this case have the following form:

$$\mathbf{M}_h = \begin{bmatrix} \cos\theta_h & -\sin\theta_h \\ \sin\theta_h & \cos\theta_h \end{bmatrix},$$

$$\mathbf{M}_k = \begin{bmatrix} \cos\theta_k & \sin\theta_k \\ -\sin\theta_k & \cos\theta_k \end{bmatrix}, \qquad (6)$$

$$\mathbf{M}_a = \begin{bmatrix} \cos\theta_a & \sin\theta_a \\ -\sin\theta_a & \cos\theta_a \end{bmatrix}.$$

The coordinates of the characteristic points of the pneumatic exoskeleton of the lower extremities, as a function of the angles (θ_h, θ_k, θ_a) can be determined from the relationship:

$$A = \begin{bmatrix} 0 \\ 0 \end{bmatrix},$$

$$B = \begin{bmatrix} (c+c^*)\tan\theta_p \\ c+c^* \end{bmatrix},$$

$$C = \begin{bmatrix} (c+c^*)\tan\theta_p + a^* \\ c \end{bmatrix},$$

$$D = \mathbf{M}_h \begin{bmatrix} l_t - a_t \\ 0 \end{bmatrix} + C,$$

$$E = \mathbf{M}_h \begin{bmatrix} l_t - a_t \\ -b_t \end{bmatrix} + C,$$

$$F = \mathbf{M}_h \begin{bmatrix} l_t - a_t \\ b_t^* \end{bmatrix} + C,$$

$$G = \mathbf{M}_h \begin{bmatrix} l_t \\ 0 \end{bmatrix} + C,$$

$$H = \mathbf{M}_h \left(\mathbf{M}_k \begin{bmatrix} a_l \\ 0 \end{bmatrix} + \begin{bmatrix} l_t \\ 0 \end{bmatrix} \right) + C,$$

$$I = \mathbf{M}_h \left(\mathbf{M}_k \begin{bmatrix} a_l \\ -b_l \end{bmatrix} + \begin{bmatrix} l_t \\ 0 \end{bmatrix} \right) + C,$$

$$J = \mathbf{M}_h\left(\mathbf{M}_k\begin{bmatrix} a_l \\ b_l^* \end{bmatrix} + \begin{bmatrix} l_t \\ 0 \end{bmatrix}\right) + C\,, \tag{7}$$

$$K = \mathbf{M}_h\left(\mathbf{M}_k\begin{bmatrix} l_l \\ 0 \end{bmatrix} + \begin{bmatrix} l_t \\ 0 \end{bmatrix}\right) + C\,,$$

$$L = \mathbf{M}_h\left(\mathbf{M}_k\left(\mathbf{M}_a\begin{bmatrix} 0 \\ -b_f \end{bmatrix} + \begin{bmatrix} l_l \\ 0 \end{bmatrix}\right) + \begin{bmatrix} l_t \\ 0 \end{bmatrix}\right) + C\,,$$

$$M = \mathbf{M}_h\left(\mathbf{M}_k\left(\mathbf{M}_a\begin{bmatrix} 0 \\ b_f^* \end{bmatrix} + \begin{bmatrix} l_l \\ 0 \end{bmatrix}\right) + \begin{bmatrix} l_t \\ 0 \end{bmatrix}\right) + C\,,$$

$$N = \mathbf{M}_h\left(\mathbf{M}_k\left(\mathbf{M}_a\begin{bmatrix} 0 \\ -b_f \end{bmatrix} + \begin{bmatrix} l_l \\ 0 \end{bmatrix}\right) + \begin{bmatrix} l_t \\ 0 \end{bmatrix}\right) + C\,,$$

$$O = \mathbf{M}_h\left(\mathbf{M}_k\left(\mathbf{M}_a\begin{bmatrix} a_f \\ l_f - b_f \end{bmatrix} + \begin{bmatrix} l_l \\ 0 \end{bmatrix}\right) + \begin{bmatrix} l_t \\ 0 \end{bmatrix}\right) + C\,.$$

Using the coordinates of geometric positions obtained from the dependence (7), the length of the muscles l_1, ..., l_6 and the length reduction coefficients ε_1, ..., ε_6 are determined. They are defined as a function of angles, hip joint θ_h, knee θ_k and ankle θ_a as:

$$\begin{aligned} &l_1(\theta_h, \theta_k, \theta_a) \\ &= \sqrt{(E(1,1) - A(1,1))^2 + (E(2,1) - A(2,1))^2} - l_{10} \\ &\vdots \\ &l_6(\theta_h, \theta_k, \theta_a) \\ &= \sqrt{(M(1,1) - J(1,1))^2 + (M(2,1) - J(2,1))^2} - l_{60} \end{aligned} \tag{8}$$

$$\varepsilon_1(\theta_h, \theta_k, \theta_a) = (l_{10} - l_1(\theta_h))/l_{10}$$

$$\vdots$$

$$\varepsilon_6(\theta_h, \theta_k, \theta_a) = (l_{60} - l_6(\theta_h))/l_{60}\,.$$

The individual values of the angles were adapted to the dependencies (7) and (8). The change in the length of the muscles during one step of walking and running was determined based on the data from IMU measurements.

3. Results

The hip, knee and ankle parameters were adapted to mathematical model as a matrix of angles vs. percentage of gait and run. In Figures 5 and 6, the simulation results are shown. Muscle lengths at rest, with a pelvic inclination angle of 12° for free walking and running, are defined as $l_{10;\ ...;60}$ = [0.38; 0.36; 0.44; 0.41; 0.28; 0.28 m]. Negative values on the graphs indicate a reduction in length (shortening of the muscle) in relation to the initial value, while positive values indicate its elongation in %. In Figure 5a, the change in hip angles and muscle length is shown based on the authors' measurement data. In the first phase, when the heel touches the ground, muscle 1 is lengthened and muscle 2 – shortened. In the middle of the cycle, both muscles are shortened, the first of which is by 8% shorter than the starting position, and the second – by 10%. At point B, the length of the first muscle is the baseline (not stretched and shortened), while the second is shortened by 7%. It is related to the forward tilt of the pelvis. It is worth noting that, in the starting position, this value was 0°. At the knee joint, the third muscle is elongated at the beginning (point *A*). The cause is in the forward limb. Thus, the fourth muscle is shortened by 5%. Characteristically, at point B, the third muscle is shortened by approximately 2.5% due to the bent knee. This is also influenced by the attachment of the third and fourth muscles below the knee joint. In Figure 5c, the change in the length of the muscles responsible for the ankle joint is illustrated. The fifth muscle (attached to the back) is shortened at the beginning due to the slope of the foot, then it increases in length and at about 50% of the stride phase is lengthened by 1%. The sixth muscle is elongated, and then it decreases in length. At about 68% of the phase of one step, its elongation reaches a maximum value of 8%. A similar situation can be observed during the run, as shown in Fig. 6. The maximum elongation ε is 11% (muscle 4 – knee joint) at 75% phase of gait.

Determining the change in the speed of muscle shortening is necessary to determine muscle parameters (pressure and the speed of filling the muscle). The change of velocity of each muscle length during walking and running is presented in Fig. 7. The continuous line marks the individual values related to gait, while the dashed line marks the speed of lengthening and shortening each muscle, expressed [m/s], during the run. The lowest values of shortening and lengthening are observed in the case of the second muscle, both for walking and running. They are respectively 0.08 and 1m/s. The highest values are characteristic of the third, fifth and sixth muscle.

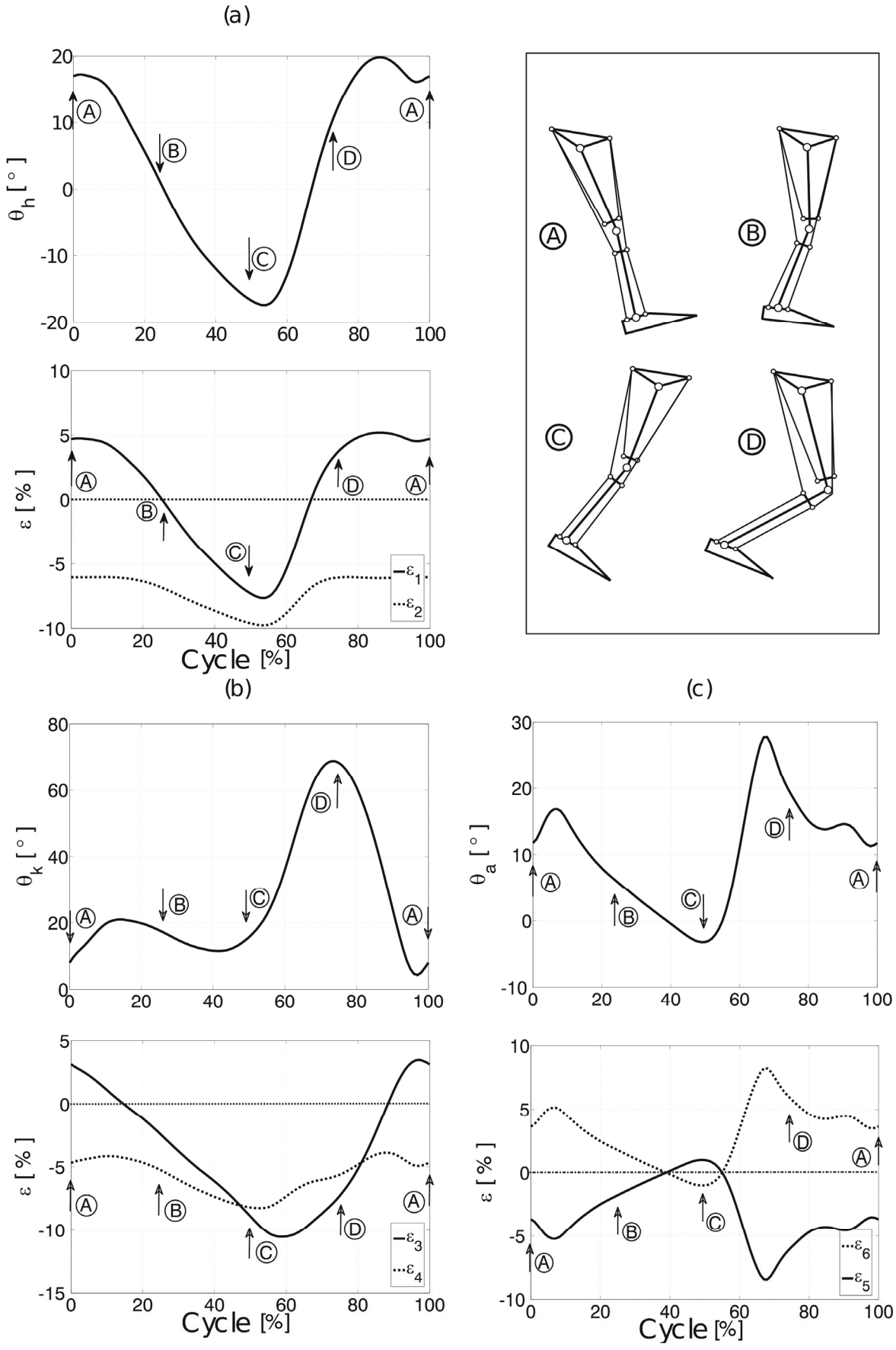

Fig. 5. (a) Change of joint angles and length of pneumatic muscles of the exoskeleton, in free gait, hip joint, (b) knee joint, (c) ankle joint

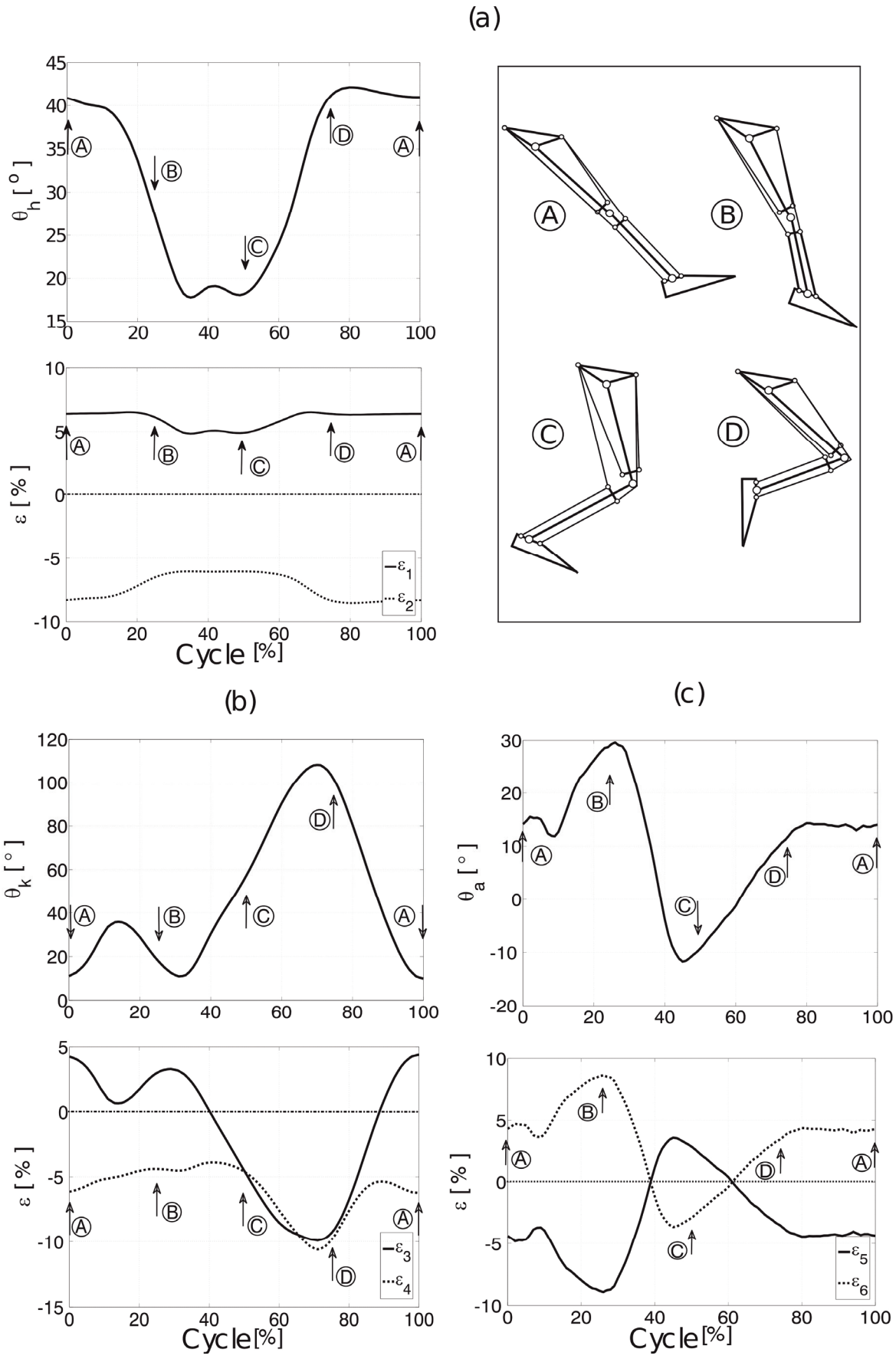

Fig. 6. (a) Change of joint angles and length of pneumatic muscles of the exoskeleton, in the run, hip joint, (b) knee joint, (c) ankle joint

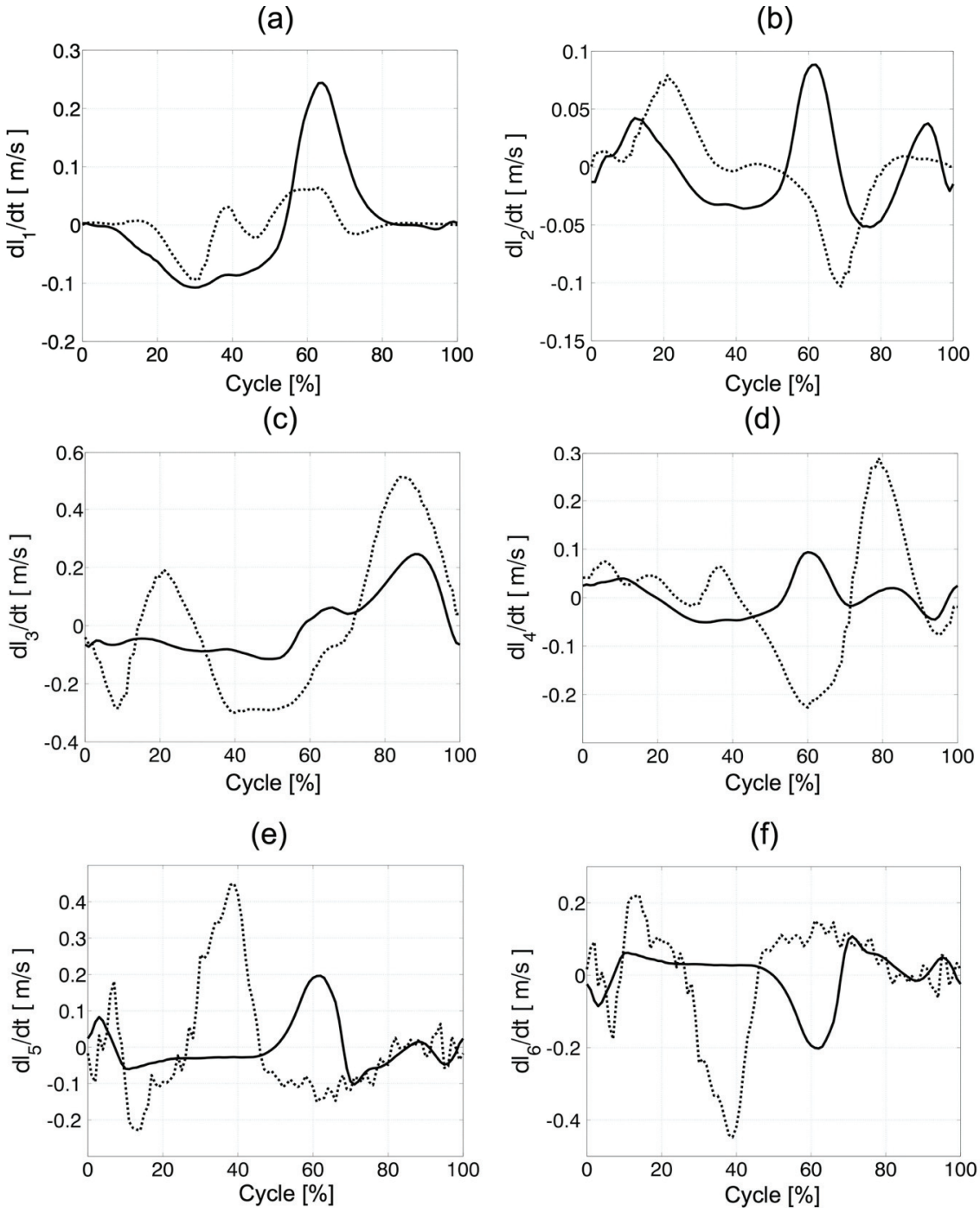

Fig. 7. Velocity of change in the length of pneumatic muscles while walking (—) and running (···) [m/s]: (a) muscle 01, (b) muscle 02, (c) muscle 03, (d) muscle 04, (e) muscle 05, (f) muscle 06

4. Discussion

The developed model can be used in the kinematic and kinetic simulation of human movement [21], [40]. The angles during walking of joints were calculated using IMUs. The use of IMUs to calculate angles is suitable for investigators because of the limited need for equipment. Unlike optical systems, they are portable, inexpensive, and testing can be done outside a laboratory. The obtained angle values can be used to determine the operating parameters of exoskeletons. IMU sensors were used to simulate walking and running. Data related to the parameters of walking and running were obtained and then used to reflect the movement of individual muscles. Next, by implementing these parameters into the model, it is possible to analyze how pneumatic artificial muscles work. Through simulation,

it is possible to determine the elongation of individual muscles. Determination of kinematic parameters enables the selection of muscles and geometric parameters.

The kinematics and the proper alignment with the corresponding joints are a central aspect of the exoskeleton's design. Improperly designed and selected operating systems of the pneumatic wearable device may have a negative impact on the user's comfort. Problems with matching the device may be related to the misalignment of the exoskeleton with individual joints. In addition, the device moves relative to the user's body during movement due to the forces occurring, which is a significant engineering challenge. Therefore, it is essential at the design stage of the exoskeleton to identify problems related to the device's design, for example, the type of actuator used (pneumatic, electric or hydraulic). Actuators introduce a significant amount of weight and inertia to the exoskeleton system to produce the physiological torques needed for the various human joints. While geared electric motors suffer from high reflected inertia and striction and are difficult to backdrive, pneumatic and hydraulic systems suffer from high friction and are very difficult to backdrive [1]. In pneumatic actuators, it is important to determine the pressure limits of each actuator design, especially when it comes to the safety of using these actuators in exoskeletons.

The proposed solutions in the form of kinematic models allow for developing a pneumatic exoskeleton. Pneumatic muscle as exoskeleton actuators are one of the most promising executive systems for rehabilitation robots, due to its inherent compliance and safety features. In recent years, there have been several well-known pneumatic muslces actuated rehabilitation robots, such as the series of upper limb exoskeleton Rupert and lower limb orthosis Kafo [10], [29]. Antagonistic configuration, as one of the most frequently used actuation schemes, can provide the bidirectional assistance to the patient's joints. One pneumatic muscles antagonistic pair consists of two muscles connected through a cable and a pulley. By regulating the pressure inside each muscle, the configuration can provide one rotational degree of freedom assistance. Hence pneumatic muscle antagonistic pairs are widely utilized in upper/lower limb multi-joint exoskeletons and to help patients to complete the assigned movement tasks [19].

Knowing the velocity of the change in the length of the artificial muscles, it is possible to select the appropriate executive system and the supply pressure of the device. If we know the parameters of human gait (IMU) by simulation, we can calculate how quickly the muscles shorten.

In skeletal muscle, the relationship between force and velocity is described by a hyperbolic function, which highlights that the force muscle fibers generate decreases with increasing speed of contraction. Experimental results show that during walking and running in the knee joint, the highest speed of shortening the pneumatic muscles is 0.5 m/s (muscle 3) and 0.3 m/s (muscle 4), respectivelly. It is influenced by the length of the thigh and lower leg, and walking speed. A reduction in pneumatic muscle shortening speed may result in a reduction in walking speed. As a rule, high speeds are not required for rehabilitation, therefore, pneumatic muscles (considering their limitations) can be successfully used for gait re-education.

To maintain a vertical position (e.g., in the case of people after a stroke), we need to build up an initial pressure on the muscles. Pneumatic muscles, McKibben as well, mimic the processes of contraction and relaxation of human muscles, causing the formation of the corresponding axial stresses. McKibben have the advantages of being lightweight, easy to fabricate, are self-limiting (have a maximum contraction) and have load-length curves similar to human muscle. This kind of muscles consist of an inflatable inner tube/bladder inside a braided mesh, clamped at the ends. When the inner bladder is pressurized and expands, the geometry of the mesh acts like a scissor linkage and translates this radial expansion into linear contraction. Additionally, they have a high power to weight ratio and power-to-volume ratio. The limitation of McKibben muscles is the non-linear relationship between stress and strain inside the inner tube elastomer. Additionally, Tondu [32] drew attention to the problem of estimate friction coefficient and its possible dependence on pressure and velocity with the weaving peculiar to McKibben braided sheaths. Theoretically, pneumatic muscles can provide safe and comfortable interaction between humans and robotic exoskeletons, but it is not always true as the energy stored in the elastic element can suddenly be released and caused to generate unsafe reaction forces [8].

This work has several limitations, for example, the IMUs system was tested only with healthy subjects in the experiments. Experiments on a larger group of people will be helpful to evaluate the performance and improve the gait kinematic parameters. An additional area of research may concern the mechanism of compensating for the misalignment of the exoskeleton and the axis of the user's knee joint. Future work shall investigate how to control the pneumatic exoskeleton.

5. Conclusions

In this paper, we presented the kinematics of exoskeleton pneumatic actuators during walk and run procees. The main aim of the research was to present a proposal for designing an exoskeleton with pneumatic actuators. We built a geometrical model of a pneumatic exoskeleton based on anthropometrical parameters. The presented results demonstrate the efficiency of the approach that can be utilized to analyze the kinematics of pneumatic exoskeletons using the devoted design process. The developed mathematical model enabled the authors to determine the position of lower limb segments and exoskeleton elements, which made it possible to calculate the position of the human leg and actuators' characteristic points. This type of exoskeleton modelling can be a popular concept, because we can change every kinematic parameter (angle, angular velocity of each joint) and observe how actuators should work. Finally, it should be noted that the proposed kinematic model of the exoskeleton may be the basis for the physical model and the analysis of gait dynamics.

References

[1] AGARWAL PRIYANSHU, DESHPANDE ASHISH A., *Exoskeletons: State-of-the-Art, Design, Challenges, and Future Directions*, Human Performance Optimization, 2018, DOI: 10.1093/oso/9780190455132.003.0011.

[2] BERBYUK V.E., LYTVYN B.A., *Mathematical modeling of human walking on the basis of optimization of controlled processes in biodynamical systems*, J. Math. Sci., 2001, 104, 1575–1586, https://doi.org/10.1023/A:1011352207020

[3] CALDWELL DARWIN G., MEDRANO-CERDA G.A., BOWLER C.J., *Investigation of bipedal robot locomotion using pneumatic muscle actuators*, Proceedings – IEEE International Conference on Robotics and Automation, 1997, 1, 799–804, DOI: 10.1109/ROBOT.1997.620132.

[4] DAERDEN F., LEFEBER D., VERRELST B., VAN HAM R., *Pneumatic artificial muscles: Actuators for robotics and automation*, International Conference on Advanced Intelligent Mechatronics, Proceedings, 2001, 2, 738–743, DOI: 10.1109/AIM.2001.936758.

[5] GŁOWIŃSKI S., KRZYŻYŃSKI T., *Modelling of the ejection process in a symmetrical flight*, Journal of Theoretical and Applied Mechanics, 2013, 51 (3), 775–785.

[6] GŁOWIŃSKI S., ŁOSIŃSKI, . ; KOWIAŃSKI P., WAŚKOW M., BRYNDAL A., GROCHULSKA A., *Inertial Sensors as a Tool for Diagnosing Discopathy Lumbosacral Pathologic Gait: A Preliminary Research*, Diagnostics, 2020, 10, 342.

[7] GŁOWIŃSKI S., OBST M., MAJDANIK S., POTOCKA-BANAŚ B., *Dynamic Model of a Humanoid Exoskeleton of a Lower Limb with Hydraulic Actuators*, Sensors, 2021, 21, 10, 3432.

[8] GROSU V., RODRIGUEZ-GUERRERO C., GROSU S., VANDERBORGHT B., LEFEBER D., *Design of smart modular variable stiffness actuators for robotic-assistive devices*, IEEE/ASME Trans. Mechatron., 2017, 22, 1777–1785.

[9] HAMDI, MOHAMMAD.; AWAD, MOHAMMED, IBRAHIM.; ABDELHAMMED, MAGDY M.; TOLBAH, FARID A.: *Lower limb gait activity recognition using Inertial Measurement Units for rehabilitation robotics*, Advanced Robotics (ICAR), 2015, DOI: 10.1109/ICAR.2015.7251474.

[10] HUANG TU X., HE J., *Design and evaluation of the RUPERT wearable upper extremity exoskeleton robot for clinical and in-home therapies*, IEEE Transactions on Systems, Man, and Cybernetics: Systems, 2016, 46, 926–935, DOI: 10.1109/TSMC.2015.2497205.

[11] HUNTER L.C., HENDRIX E.C., DEAN J.C., *The cost of walking downhill: Is the preferred gait energetically optimal?*, Journal of Biomechanics, 2010, 43 (10), 1910–1915, DOI: 10.1016/j.jbiomch.2010.03.030.

[12] Inertia Technology: *ProMove MINI*, URL https://inertia-technology.com/product/motion-capture-promove-mini/ (Accessed: 10.06.2021).

[13] JACOB, CAROLINE E.M. ; KLUGE F., KUGLER P.F.-X., *Estimation of the Knee Flexion-Extension Angle During Dynamic Sport Motions Using Body-worn Inertial Sensors*, BodyNets 13 Proceedings of the 8th International Conference on Body Area Networks, 2013, 289–295, https://doi.org/10.4108/icst.bodynets.2013.253613

[14] KAZEROONI H., STEGER R., HUANG LIHUA, *Hybrid control of the Berkeley Lower Extremity Exoskeleton (BLEEX)*, International Journal of Robotics Research, 2006, 25, https://doi.org/10/1177/0278364906065505

[15] KOBIELARZ M., SZOTEK S., GŁOWACKI M., DAWIDOWICZ J., PEZOWICZ C., *Qualitative and quantitative assessment of collagen and elastin in annulus fibrosus of the physiologic and scoliotic intervertebral discs*, J. Mech. Behav. Biomed. Mater., 2016, 62, 45–56, DOI: 10.1016/j.jmbbm.2016.04.033.

[16] LAROCHE, DAIN P. ; COOK, SUMMER B., MACKALA K., *Strength Asymmetry Increases Gait Asymmetry and Variability in Older Women*, Med. Sci. Sport. Exerc., 2012, 44, 11, 2172–2181, DOI: 10.1249/MSS.0b013e31825e1d31.

[17] LECLAIR J., PARDOEL S., HELAL A., DOUMIT M., *Development of an unpowered ankle exoskeleton for walking assist*, Disabil. Rehabil. Assist. Technol., 2020, 15 (1), 1–13, DOI: 10.1080/17483107.2018.1494218.

[18] LI I. HSUM; LIN, YI SHAN ; LEE, LIAN WANG; LIN, WEI TING: *Design, manufacturing, and control of a pneumatic-driven passive robotic gait training system for muscle-weakness in a lower limb*, Sensors, 2021, 21 (20), 6709, DOI: 10.3390/s21206709.

[19] LIU Q., ZUO J., ZHU C., XIE S.Q., *Design and control of soft rehabilitation robots actuated by pneumatic muscles: State of the art*, Future Generation Computer Systems, 2020, 113, 620–634, https://doi.org/10/1016/j.future.2020.06.046

[20] MACKAY G., *Injury to pedestrians*, A Rep. Road Accid. Res. Proj. to Sci. Res. Counc., 1972, 3, 1–26.

[21] MILANOWSKI H., PILAT A., *Comparison of Identified and SimScape Model of Human Leg Motion*, 2020 International Conference Mechatronic Systems and Materials (MSM), IEEE, 2020 – ISBN 978-1-7281-6956-9, 1–6, DOI: 10.1109/MSM49833.2020.9201736.

[22] NORRIS J.A., GRANATA K.P., MITROS M.R., BYRNE E.M., MARSH A.P., *Effect of augmented plantarflexion power on preferred walking speed and economy in young and older adults*, Gait and Posture, 2007, 35 (4), 620–627, DOI: 101016/j.gaitpost.2006.07.002.

[23] ONYSHKO S., WINTER D.A., *A mathematical model for the dynamics of human locomotion*, J. Biomech., 1980, 13, 4, DOI: 10.1016/0021-9290(80)90016-0.

[24] PETRE I., DEACONESCU A., ROGOZEA L., DEACONESCU T.I., *Orthopaedic Rehabilitation Device Actuated with Pneumatic Muscles*, International Journal of Advanced Robotic Systems, 2014, https://doi.org/10.5772/58693.

[25] PONS J.L. (Ed.), *Wearable Robots*, John Wiley & Sons, Ltd., Chichester, UK, 2008, ISBN 9780470987667.

[26] PTAK M., *Pedestrian safety: a new method to assess pedestrian kinematics*, Transport, 2019, 34, 41–51.

[27] ROCON E., PONS J.L., *Exoskeletons in Rehabilitation Robotics*, *Springer Tracts in Advanced Robotics*, 69. Berlin, Heidelberg, Springer, Berlin–Heidelberg, 2011, ISBN 978-3-642-17658-6.

[28] ROJEK A., MIKA A., OLEKSY Ł., STOLARCZYK A., KIELNAR R., *Effects of Exoskeleton Gait Training on Balance, Load Distribution, and Functional Status in Stroke: A Randomized Controlled Trial*, Front. Neurol., 2020, 10, 1344, DOI: 10.3389/fneur.2019.01344.

[29] SAWICKI G.S., FERRIS D.P., *A pneumatically powered knee-ankle-foot orthosis (KAFO) with myoelectric activation and inhibition*, J. Neuroeng. Rehab., 2009, 6, 23–29, DOI: 10.1186/1743-000306-23.

[30] SHAHEEN R., DOUMIT M., HELAL A., *Design and characterization of a hyperelastic tubular soft composite*, J. Mech. Behav. Biomed. Mater., 2017, 75, 228–235, DOI: 10.1016/j.jmbbm.2017.07.031.

[31] SHORTER K.A., KOGLER G.F., LOTH E., DURFEE W.K., HSIAO-WECKSLER E.T., *A portable powered ankle-foot orthosis for rehabilitation*, J. Rehabil. Res. Dev., 2011, 48 (4), 459–472, DOI: 10.1682/jrrd.2010.04.0054.

[32] TONDU B., *Modelling of the McKibben artificial muscle: A review*, Journal of Intelligent Material Systems and Structures, 2012, 23 (3), 225–253, DOI: 10.1177/1045389X11435435.

[33] VALAYIL, TONY PUNNOOSE; AUGUSTINE, ROSE SHAJI., *Kinematics and workspace analysis of a robotic device for performing rehabilitation therapy of upper limb in stroke-affected patients*, Acta of Bioeng. Biomech., 2021, 23 (3), 175–189, PMID: 34978313.

[34] VAUGHAN C.L., *Biomechanics of running gait*, Crit. Rev. Biomed. Eng., 1984, 12 (1), 1–48, PMID: 6394212.

[35] VEALE, ALLAN JOSHUA ; XIE, SHANE QUAN, *Towards compliant and wearable robotic orthoses: A review of current and emerging actuator technologies*, Med. Eng. Phys., 2016, 38 (4), 317–325, DOI: 10.1016/j.medengphy.2016.01.010.

[36] WOERNLE C., *Med. Mehrkörpersysteme: Eine Einführung in die Kinematik und Dynamik von Systemen starrer Körper*, *Springer*, 2011, ISBN-10:3662466864.

[37] WU GE, SIEGLER SORIN, ALLARD P., KIRTLEY C., LEARDINI A., ROSENBAUM D., WHITTLE M., D'LIMA D.D., *ISB recommendation on definitions of joint coordinate system of various joints for the reporting of human joint motion* – part I: *ankle, hip, and spine*, J. Biomech., 2002, 35 (4), 543–548, DOI: 10.1016/s0021-9290(01)00222-6.

[38] YE, XIN ; CHEN, CHUNJIE; SHI, YANGUO; CHEN, LINGXING; WANG, ZHUO; ZHANG, ZHEWEN; LIU, YIDA; WU, XINYU, *A Time Division Multiplexing Inspired Lightweight Soft Exoskeleton for Hip and Ankle Joint Assistance*, Micromachines, 2021, 12 (10), 1150, DOI: 10.22290/mi12101150.

[39] ZHANG, JIA FAN; YANG, CAN JUN; CHEN, YING; ZHANG, YU; DONG, YI MING, *Modeling and control of a curved pneumatic muscle actuator for wearable elbow exoskeleton*, Mechatronics, 2008, 18 (8), 448–457, DOI: 10.1016/j.mechatronics.2008.02.006.

[40] ŻUK M., PEZOWICZ C., *Kinematic Analysis of a Six-Degrees-of-Freedom Model Based on ISB Recommendation: A Repeatability Analysis and Comparison with Conventional Gait Model*, Appl. Bionics Biomech., 2015, 503713, DOI: 10.1155/2015/503713.